Sensors and Materials, Vol. 38, No. 4 (2026) 2217–2232
MYU Tokyo

S & M 4432

Advanced Noninvasive Capacitive Coupling Sensors for Online Frequency-modulated Continuous-wave-based Localization of Insulation Defects in Cross-linked Polyethylene Cables

Dewen Zhang,* Hang Lu, Ruihui Han, Jie Sheng, Zhongyu Wang, and Chao Xu

Economic and Technical Research Institute, State Grid Heilongjiang Electric Power Co., Ltd., Harbin, Heilongjiang Province 150000, China

(Received January 29, 2026; accepted April 3, 2026)

Keywords: FMCW, distribution cables, capacitive coupling

Cross-linked polyethylene (XLPE) cables are essential in modern power distribution, yet insulation defects such as localized aging, moisture ingress, and sheath damage threaten grid reliability. Conventional diagnostic methods, including time-domain reflectometry and broadband impedance spectroscopy, lack resolution or require outages, limiting their use in live systems. To overcome these challenges, we developed an advanced online defect localization system, employing frequency-modulated continuous-wave signals with a novel noninvasive capacitive coupling sensor. To mitigate signal attenuation caused by metallic shielding, a specialized hardware interface and a selective shielding removal strategy were implemented. Experimental results demonstrated high spatial accuracy: transmission distances of 97.3 and 101.26 m matched physical cable lengths under core-conductor and optimized capacitive coupling configurations. Capacitive and inductive sensor data exhibited a 4.46% difference in transmission speeds, highlighting distinct coupling characteristics. The system developed in this study successfully localized a 2 m thermal aging defect at 41 m along a 64 m cable, with only 5.10% relative error. Furthermore, notch peak intervals were shown to characterize defect severity, while single-cycle signal mixing mitigated harmonic interference, producing smoother spectral curves. By translating longitudinal delays into frequency differences, the system can be used to develop cable diagnostics from passive monitoring to active, high-resolution live-line detection, laying the foundation for intelligent sensor technologies in smart grid infrastructure.

1. Introduction

With the acceleration of global urbanization, cross-linked polyethylene (XLPE) cables have become the backbone of power transmission and distribution networks,[1,2] owing to their excellent insulation, high reliability, and compact footprint.[3] However, a significant portion of these distribution cables is exposed to complex underground and atmospheric environments for extended periods, making them susceptible to insulation defects.[4,5] These defects might cause

*Corresponding author: e-mail: dewen1984@163.com
https://doi.org/10.18494/SAM6265

ISSN 0914-4935
https://myukk.org/

catastrophic power system failures, significantly threatening the operational stability of smart grids.[6,7]

To reduce such risks, robust sensing and monitoring technologies, such as time-domain reflectometry (TDR) and frequency-domain reflectometry (FDR), have been introduced.[8,9] Recently, frequency-modulated continuous-wave (FMCW) methods have come to be regarded as high-performance cable diagnostic methods. By utilizing a frequency-sweeping sensing signal and extracting the longitudinal frequency difference between incident and reflected waves, FMCW methods ensure superior noise immunity and extended detection ranges compared with traditional broadband impedance spectroscopy (BIS).[10,11] Despite its advantages, existing FMCW sensing systems are limited to offline power outages. In urban areas, arranging scheduled outages for cable testing is increasingly difficult as it requires a method to transition from passive, offline testing to active, online sensor systems capable of live detection under live operating conditions.

Cable diagnostics can be broadly categorized into passive and active methods. Passive monitoring, such as partial discharge detection, is widely used for live-line systems to identify defects once insulation degradation has reached a critical stage where discharges occur.[12] Active methods using reflectometry are used to proactively probe the cable's impedance profile to identify nascent soft faults, such as thermal aging, which do not cause discharge events.[13]

Among the currently used techniques, FMCW reflectometry provides higher spatial resolution and better noise rejection than traditional TDR by translating longitudinal delays into frequency differences. However, high-resolution active detection has traditionally required offline outages for direct signal injection to penetrate metallic shielding. While researchers have explored nonintrusive inductive coupling for live-line diagnostics, limited resolution and high signal attenuation still need to be addressed.[14]

Therefore, we investigated the hardware and signal-processing bottlenecks that hinder live cable monitoring using advanced sensor technologies. To enable noninvasive signal injection under energized conditions, we integrated high-frequency current-transformer (HFCT) sensors with capacitive coupling interfaces. This configuration supports the development of a live-line FMCW diagnostic system that preserves a high signal-to-noise ratio (SNR) even in the presence of strong electromagnetic interference from the power grid. In addition, we designed a dedicated data-processing module to compensate for impedance variations introduced by connected electrical equipment, thereby enhancing the adaptability and intelligence of the sensing chain. By introducing a novel noninvasive capacitive coupling sensor and optimizing both the hardware interface and shielding removal methodology, the system developed in this study achieves the high-resolution active monitoring of distribution cables under live-line operation without requiring power interruption. The system demonstrates localized defect detection with a relative error of 5.10%, representing a significant advancement in online monitoring capabilities and marking a step toward intelligent, adaptive power cable diagnostics.

2. Literature Review

2.1 Evolution of reflectometry-based sensing

Cable defect sensing is conducted to identify impedance discontinuities. TDR is the most widely used sensing method, but it shows low resolution and susceptibility to interference.[15] FDR addresses these issues by enabling noise immunity through the analysis of frequency-domain characteristics of reflected signals. In reflectometry-based cable diagnostics, interference and reflection are considered the boundary reflections that define the sensing environment. Interference refers to the near-end reflection occurring at the interface between the signal injection sensor, such as a capacitive coupler or HFCT, and the cable terminal. Interference creates a blind zone that masks defects located in proximity to the source.[16] In contrast, reflection represents the far-end reflection originating from the cable termination or the impedance mismatch caused by connected grid equipment such as transformers and busbars.[17] In live-line FMCW sensing, the challenge lies in distinguishing the low-amplitude reflections of an insulation defect from these high-magnitude boundary signals, which can cause spectral leakage and obscure the sensor's accuracy. Zhao *et al.* applied FMCW to enhance the performance of FDR.[10] By injecting a frequency-swept signal whose modulation is a linear function of time, their system extracted electrical information to identify defects.[18] By converting amplitude measurements into longitudinal frequency differences, the method extends the monitoring range to beyond 800 m, which shows a 33% improvement over conventional BIS techniques.[19] Furthermore, it enables integrated sensing for the continuous monitoring of cable conditions.

2.2 Sensor hardware and system architecture

An FMCW-based sensing system consists of (1) a signal module that generates the continuous linear frequency-modulated chirp, (2) a transmission and coupling module employing a power splitter and circulator to direct signals, and (3) a data processing module that demodulates signals by fast Fourier transform. However, the current model relies largely on offline data acquisition and post-processing under controlled conditions. To enable live detection in practical environments, additional sensors are required to improve the SNR, along with coupling algorithms that support real-time signal integration.

2.3 Sensor technology under live conditions

Implementing sensors on live distribution cables faces several challenges. Operating cables are surrounded by power-frequency electromagnetic fields and harmonics, which suppress conventional sensor signals.[20] To overcome these limitations, a coupling mechanism is required to safely inject sensing signals into high-voltage cables and mitigate suppression effects. Two sensor coupling technologies are employed for signal-to-cable integration. In electromagnetic (inductive) coupling, HFCTs are widely used. Although effective, this approach is limited by

shielding effects from metallic cable layers and by eddy current losses.[21] In contrast, capacitive coupling provides strong penetration through metallic conductors and exhibits exceptionally high noise immunity. As it does not induce eddy current losses, energy dissipation during signal transmission is minimal.[22]

Despite the potential of FMCW sensing, the influence of cable-connected electrical equipment, such as transformers, on localization accuracy under live operating conditions has not been extensively explored. Therefore, we examined the combined effect of HFCT and capacitive coupling sensors to develop a robust live sensing system for distribution cables.

2.4 FMCW signal modulation and detection

The localization of partial insulation defects based on FMCW is an advanced FDR method. This method involves the injection of a linear frequency-modulation (LFM) sweep signal into the cable. By mixing the incident and reflected signals, the method extracts the cable's electrical characteristics to identify impedance discontinuities. While traditional BIS is used to measure magnitude directly, FMCW is used to translate the longitudinal delay of the signal into a distinct frequency difference. This translation enhances noise immunity and detection sensitivity, enabling a broader diagnostic range for localized defects.[18,19] This method has been developed on the basis of the stepped-frequency continuous wave (SFCW) method. While SFCWs improve measurement efficiency by utilizing segmented sweeping and reducing testing intervals to under 10 s, their application is constrained by hardware-limited frequency steps. The recent FMCW method overcomes these limitations, providing high-resolution localization spectra for preventive maintenance before a full insulation breakdown occurs.

The deployment of FMCW sensing in live environments introduces electromagnetic interference in the presence of power-frequency fields and harmonic noise, which significantly degrades the SNR of traditional reflectometry. In addition, safe signal injection into high-voltage conductors requires noninvasive interfaces. In this study, we evaluated HFCT inductive coupling and capacitive coupling for extracting weak defect reflections from live distribution lines.

3. Methods

3.1 System architecture

It is necessary to differentiate the physical capacitive coupling sensor from the integrated online sensing system to ensure the reproducibility of fault detection. The capacitive coupling sensor is the ring-shaped electrode that facilitates the signal transition via displacement current.[13] The sensing system integrates this sensor with an LFM generator and a digital acquisition interface. The sensor used in this study was fabricated using 0.1-mm-thick flexible copper foil. To test the 10 kV XLPE cable, the electrode was designed with a width of 80 mm, providing a calculated coupling capacitance of approximately 15–25 pF depending on the dielectric thickness of the cable jacket.[23] The hardware interface connecting the signal generator to the sensor includes a protection module consisting of a 20 pF/15 kV coupling

capacitor and a 50 Ω matching resistor to minimize signal reflections at the high-frequency range (1–40 MHz).[24] To enable signal injection into the shielded cable, a 100 mm section of the metallic sheath was removed at the injection point, while maintaining the continuity of the ground path through an external bypass wire.

3.2 Online localization and capacitive interface

The defects found in cables primarily include dendritic degradation structures known as trees. These trees are categorized into water trees, which are initiated by the combined action of moisture and electric stress originating from contaminants or voids, and electrical trees. The latter consist of permanent carbonized channels formed by persistent partial discharge (PD) activity, which ultimately leads to catastrophic dielectric failure.[25] In addition to trees, other common insulation anomalies include internal voids (microscopic gas pockets), moisture ingress (localized high-permittivity zones), and thermal degradation (chemical aging of the polymer chains).[25]

While the proposed FMCW system excels at localizing these defects by identifying impedance discontinuities, defect types are detected by analyzing the reflection coefficient's spectral signature. Specifically, the notch features are identified to provide a metric for defect severity, integrating phase-based impedance spectroscopy to enhance defect classification accuracy.[26] However, distinguishing between a water tree and a localized void currently relies on the magnitude of the impedance change, which is monitored using a phase-based impedance spectroscopy to enhance defect classification accuracy.

In this study, a specialized capacitive coupling hardware interface was developed. The interface employs a sensor designed to inject high-frequency FMCW signals into the cable while effectively blocking the 50/60 Hz power-frequency voltage. The experimental system architecture comprises a signal generation module to produce an LFM sweep signal, a coupling sensor to ensure uniform electromagnetic field distribution during signal injection using a ring-shaped capacitive electrode, and a standard XLPE cable to evaluate the spatial accuracy of the localization method (Fig. 1).

Figure 2 shows the schematic of the HFCT-based signal injection/detection approach, showing the placement of HFCT sensors at both the injection and detection ends of the cable,

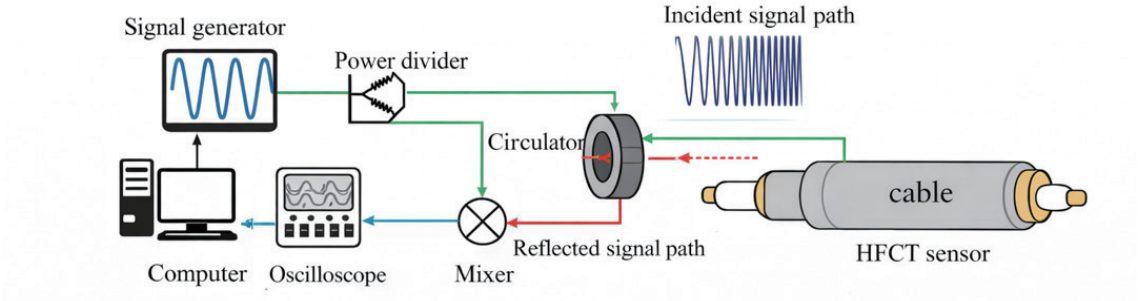

Fig. 1. (Color online) Diagram of FMCW live detection of cable defects.

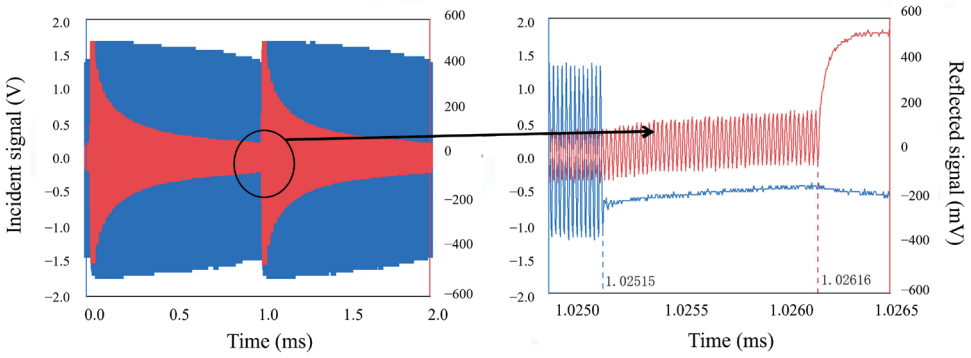

Fig. 2. (Color online) Incident and reflected signals from offline FMCW cable defect localization experiment.

along with the signal generator, circulator, mixer, and oscilloscope modules. This complementary schematic enhances readability by clarifying the differences between capacitive and inductive coupling configurations. HFCTs are widely employed for noninvasive signal injection and detection in energized cables. HFCTs operate on the principle of inductive coupling, where a toroidal magnetic core encircles the cable conductor to sense displacement currents induced by the injected FMCW signal. Whereas capacitive coupling relies on displacement current through an electrode interface, HFCTs detect the magnetic field generated by high-frequency currents flowing through the conductor. The injection process involves placing the HFCT around the cable at the head-end, where the modulated FMCW signal is introduced. The reflected signal, carrying impedance discontinuity information, is retrieved at the terminal end using another HFCT sensor. The inductive coupling mechanism provides galvanic isolation and avoids direct contact with the conductor, making it suitable for live-line applications. However, HFCTs are more susceptible to shielding effects and eddy current losses in metallic layers, which can attenuate the transmitted signal and reduce spatial resolution compared with capacitive coupling.[27]

To investigate FMCW signal transmission and the influence of the coupling interface, eight experimental configurations were established. These configurations varied in accordance with the signal injection method (core conductor vs capacitive coupling) and the acquisition method at both the head-end and terminal-end of the cable (Table 1).

Signal processing involved mixing incident and reflected LFM waveforms to extract spectral features. By translating the longitudinal time delay of the reflected signal into a frequency difference, the system identifies impedance discontinuities corresponding to cable terminations or insulation defects. Theoretical frequency shifts were calculated using the signal propagation velocity and modulation parameters.

On the basis of the initial experimental results, to mitigate the cable's copper shielding attenuated signals injected using capacitive coupling, the insulation, copper shielding, and semiconductive layers were removed at the coupling points. Under such optimized conditions, the following two coupling methods were compared.

- Ring-shaped capacitive coupling was assessed for its high noise immunity and absence of eddy current losses.

Table 1
Experimental results of FMCW sweep signal transmission in cables.

Configuration	Injection method	Detection method (head end)	Detection method (terminal end)	Existence of time difference (time domain)	Frequency difference (frequency domain)
1	Core conduction	Capacitive coupling	Capacitive coupling	Yes, 568.0 ns	29000 Hz
2	Core conduction	Capacitive coupling	Capacitive coupling	Minimal, 26.07 ns	No distinct characteristic peak
3	Core conduction	Capacitive coupling	Core conductor	Yes, 551.9 ns	27000 Hz
4	Core conduction	Core conductor	Capacitive coupling	Minimal, 24.46 ns	No distinct characteristic peak
5	Capacitive coupling	Core conductor	Core conductor	Minimal, 21.66 ns	No distinct characteristic peak
6	Capacitive coupling	Capacitive coupling	Capacitive coupling	Minimal, 30.68 ns	No distinct characteristic peak
7	Capacitive coupling	Core conductor	Capacitive coupling	Minimal, 10.23 ns	No distinct characteristic peak
8	Capacitive coupling	Capacitive coupling	Core conductor	Minimal, 22.68 ns	No distinct characteristic peak

- HFCT was assessed as an inductive coupling alternative to compare transmission speed and localization accuracy.

We detected simulated thermal aging defects under live operating conditions. A 2.5 V FMCW sweep signal was applied across a frequency range of 1 μHz to 40 MHz with a modulation period of 1 ms. Signals were injected and retrieved at the cable head-end via the capacitive coupling interface. Following mixing, the resulting spectrum was analyzed for notch features, which indicate reflections caused by insulation degradation. The presence of these spectral notches confirmed the effectiveness of the FMCW-based online localization method under capacitive coupling.

3.3 Measurement

To evaluate the efficacy of the proposed system, offline and online measurement protocols were employed on XLPE cable specimens (YJV-8.7/10 kV × 300 mm) (copper conductor, XLPE insulation, polyethylene sheath, rated for 8.7/10 kV AC, and a cross-section of 300 mm^2) of 64 and 99 m lengths. The offline measurements were conducted to determine the maximum achievable resolution without the influence of grid noise or coupling loss. In offline measurement, the cable was disconnected from the power source, and the FMCW signal was injected directly into the conductor through a coaxial interface. This configuration utilized a standard vector network analyzer or a high-speed digital-to-analog converter to maintain a strictly controlled impedance environment.[28]

For online measurements, the cable was connected to the distribution system. The signal was injected via the ring-shaped capacitive coupling sensor. To protect the low-voltage signal generation hardware from the high-voltage power line, a specialized interface consisting of a 20

pF ceramic coupling capacitor and a high-pass filter (cut-off frequency of 100 kHz) was used. Data were acquired using a high-resolution oscilloscope synchronized with the start of the FMCW sweep. To mitigate the impact of the power-frequency voltage and industrial noise, a temporal averaging technique (N = 128) was applied to the captured waveforms before performing the fast Fourier transform for localization.[29] The relative error and sensitivity were then calculated by comparing these online results with the offline baseline data.

4. Results

4.1 Localization failure

Experimental measurements revealed notable spectral fluctuations at the cable termination point. However, no discernible localization peaks indicative of insulation defects were detected. Additionally, the absence of the characteristic far-end reflection signature hindered the accurate spatial calibration of the measurement system.[30] To assess system performance, a comparative analysis was conducted using offline experimental data. In the offline configuration, a distinct time delay between the incident and reflected FMCW signals was observed, enabling the reliable identification and localization of cable anomalies. In contrast, the online measurement data exhibited minimal temporal separation between the transmitted and received signals. The lack of separation suggests that the received signal is significantly influenced by direct reflection artifacts originating from the ring-shaped capacitive coupling interface. Under the current capacitive injection conditions, the strong interface reflections suppress the low-amplitude signals that carry information about the cable's internal structure. As a result, defect localization is compromised owing to the suppression of diagnostically relevant reflections.

Signal injection into the cable was performed using a circular coupling capacitor, and the reflected signal was processed through a mixer to extract spectral features. Despite the presence of significant spectral variations at the cable input, no distinct localization peaks were observed. Furthermore, the absence of the terminal reflection peak rendered precise spatial referencing infeasible. Figure 2 highlights the temporal separation and defect-induced reflections, providing a baseline for identifying impedance discontinuities in the absence of online interface artifacts. It also shows the incident and reflected waveforms obtained from the offline FMCW cable defect localization experiment, where temporal separation and defect-induced reflections are clearly distinguishable.

4.2 Comparison of signal transmission methods

To investigate the transmission behavior of FMCW signals in cables, eight experimental configurations were designed by varying the signal injection method and the signal acquisition method. The comparative results are summarized in Table 1. The analysis results showed that characteristic peaks, corresponding to time-delay and frequency-shift signatures of the transmission process, were extracted only when terminal detection employed the core conductor

(Configurations 1 and 3). In contrast, configurations relying solely on capacitive detection failed to produce distinct localization peaks.

In Configurations 2 and 4–8, the measured time differences were minimal, with an average time difference of 22.63 ns. This suggests that signals injected via capacitive coupling are substantially attenuated by the cable's copper shielding, limiting access to internal transmission characteristics. In contrast, Configuration 1, with core conductor injection and detection, exhibited a distinct time delay of approximately 568.0 ns. Using the signal propagation velocity, the corresponding transmission distance was calculated to be 97.3 m, which accurately matches the physical cable length. The theoretical frequency shift was computed as follows.

$$551.9\ \text{ns} \times \frac{50\ \text{MHz}}{1\ \text{ms}} = 27595\ \text{Hz} \tag{1}$$

The experimentally observed peak at 27000 Hz deviated by 2.2%, confirming the validity of the measurement. However, capacitive coupling introduced multiple interference peaks, indicating signal distortion. The waveforms demonstrate time-of-flight delays achieved through core conductor injection and detection, validating signal integrity when shielding attenuation is bypassed (Fig. 3).

4.3 Mitigation of shielding effects and coupling comparison

To reduce the attenuation caused by the cable's shielding, the insulation, copper shielding, and semiconductive layers were removed at the coupling points. Figure 4 shows the selective removal of the outer insulation, copper shielding, and semiconductive layers required to mitigate signal suppression and optimize capacitive injection. Figure 4(a) shows the cable with its outer insulation and shielding layers removed, exposing the inner dielectric and conductor for direct capacitive coupling, whereas Figs. 4(b) and 4(c) show the cable wrapped in braided copper shielding to introduce attenuation and eddy current losses during signal injection, and the cable covered with a semiconductive layer to partially suppress high-frequency signals and affect

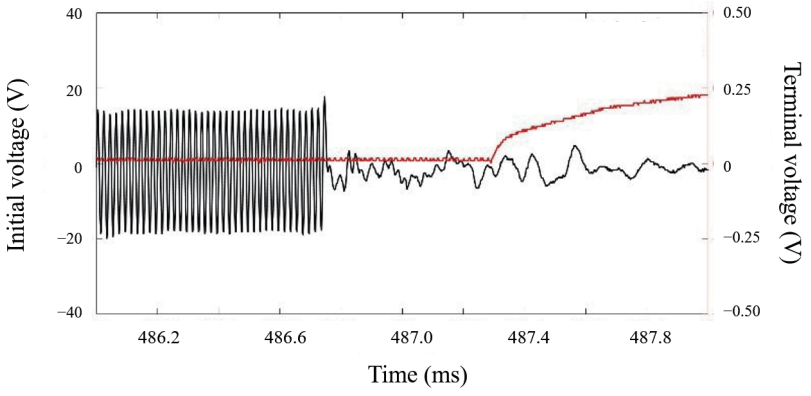

Fig. 3. (Color online) Signal acquisition at the head and terminus of cable for Configuration 3.

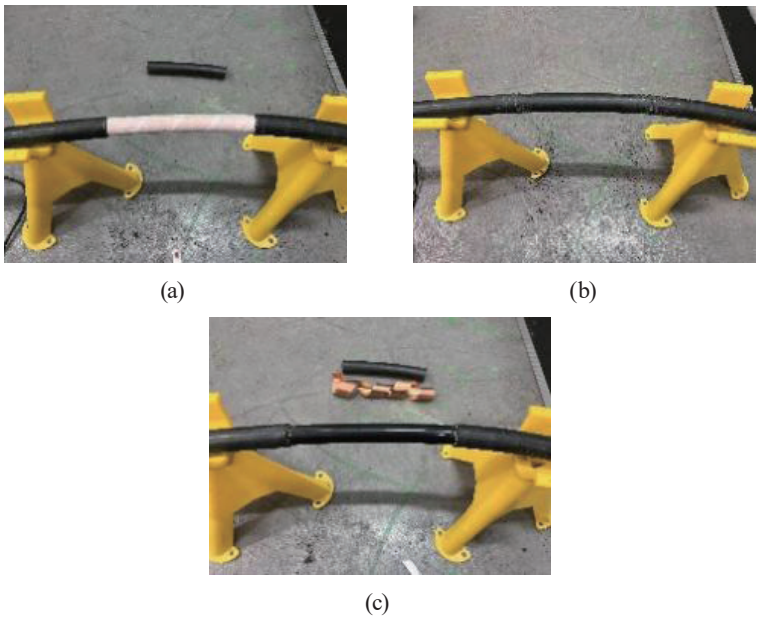

Fig. 4. (Color online) Coupling points (a) without shielding, (b) with copper shielding, and (c) with semiconductive layers.

coupling efficiency. Following the removal, two coupling methods, ring-shaped capacitive coupling and HFCT, were evaluated.

When using ring-shaped capacitive coupling, a distinct time delay of 574.4 ns was observed between the cycle endings of the two signal groups. From the calculated wave propagation speed of 1.763×10^8 m/s, the corresponding transmission distance was determined to be 101.26 m. This result aligns closely with the expected cable length, confirming that the observed time delay accurately represents the signal transmission time between the cable terminals.

In the HFCT method, a clear time delay of 548.7 ns was measured, yielding a calculated transmission distance of 96.74 m. This value also corresponds well with the physical cable length, thereby validating the accuracy of the HFCT-based measurement. Both methods successfully demonstrated the normal signal transmission process within the cable. The difference of 4.46% between the two results is attributed to differences in coupling mechanisms, with the HFCT method exhibiting slightly faster transmission than capacitive coupling.

4.4 Online localization of cable terminals and defects

Online terminal localization experiments were conducted on a 99 m cable with the shielding layer removed, using the capacitive coupling method. Under dual-cycle signal mixing, distinct notch characteristics were observed at 43500 and 54000 Hz in the 40 and 50 MHz frequency bands, respectively. The relative errors compared with theoretical values were 5.34 and 5.92%, and the reflection peak from the cable end was successfully identified. The corresponding spectrum for online localization of the cable terminal by capacitive coupling and FMCW (40 MHz sweep) is shown in Fig. 5.

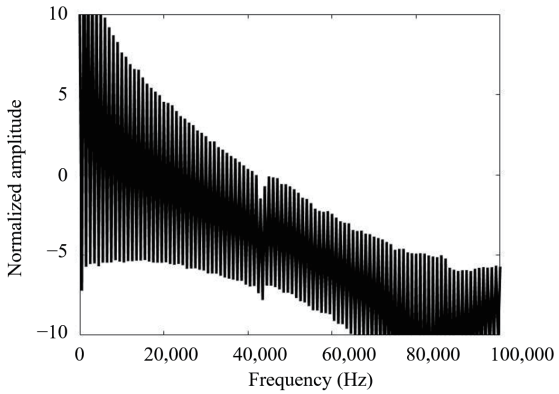

Fig. 5. Notch features at frequencies corresponding to terminal impedance mismatch for precise spatial calibration.

Next, the single-cycle signal mixing process was adopted. In the process, the positions of the notch peaks remained consistent, while the spectral curves became smoother and easier to interpret. This improvement in readability was achieved at the expense of reduced noise immunity. The single-cycle FMCW signal mixing process involves processing signals within a 1 ms integration interval. The localization results under the two frequency bands are presented in Fig. 6, which illustrates the online localization spectrum (40 MHz sweep) of the cable terminal with capacitive coupling and FMCW. The experimental results deviated by 969 Hz from the theoretical calculation, corresponding to a relative error of 5.10%. Despite this deviation, the identified notch peaks accurately represented reflections caused by insulation degradation. These results confirm the effectiveness of the proposed FMCW-based online localization method under capacitive coupling.

4.5 Online localization of thermal aging defects

On the basis of the preceding experimental results, an online localization experiment was conducted to identify thermal aging defects in a 64 m YJV-8.7/10 kV × 300 distribution cable. A 2 m thermal aging defect was emulated at the 41 m position using heating tapes and specialized wrapping materials, as shown in Fig. 7.

For detection, a 2.5 V FMCW sweep signal was applied across a frequency range of 1 μHz to 40 MHz with a modulation period of 1 ms. The signal was injected and retrieved at the cable head-end via a capacitive coupling interface. During subsequent mixing, incident and reflected signals were acquired over a 2 ms interval, corresponding to two complete signal cycles. The resulting spectrum, reflecting the cable's internal impedance characteristics, is presented in Fig. 8.

Spectral analysis revealed distinct notch features at 20000 and 22000 Hz. This dual-peak response is attributed to reflections generated by the 2 m longitudinal span of the defect. The theoretical frequency difference for this defect position was calculated as follows.

$$574.4\ \text{ns} \times \left(\frac{41}{64}\right) \times 2 \times \frac{40\ \text{MHz}}{1\ \text{ms}} = 19031\ \text{Hz} \tag{2}$$

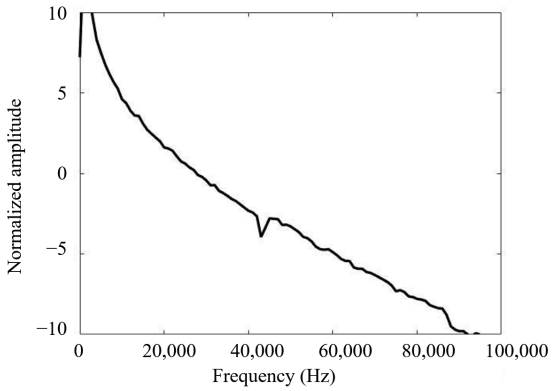

Fig. 6. Spectral response of 99 m cable terminal utilizing single-cycle mixing.

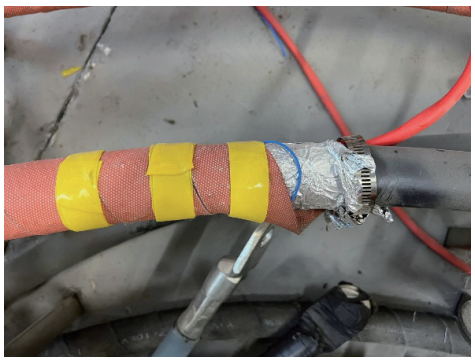

Fig. 7. (Color online) Thermal aging defect emulated on cable.

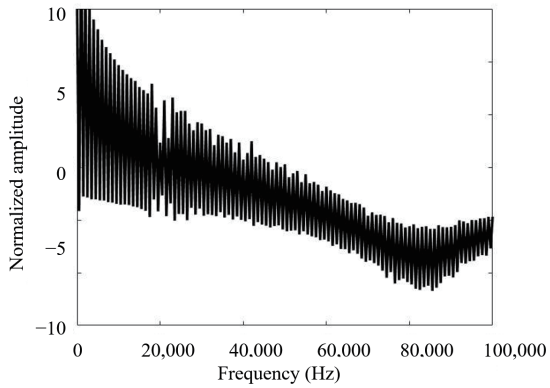

Fig. 8. Localization spectrum of thermal aging defect using online capacitive coupling (40 MHz sweep).

The experimental result deviated by 969 Hz from the theoretical value, corresponding to a relative error of 5.10%. Despite this minor discrepancy, the identified notch peaks accurately represent reflections caused by insulation degradation. These findings confirm the effectiveness of the FMCW-based online localization method under capacitive coupling for detecting thermal aging defects in high-voltage distribution cables.

5. Discussion

The results of this study provide a basis for the transition from passive, offline cable diagnostics to active, online sensor systems for smart grid infrastructure. The evaluation results of FMCW signal processing in different coupling interfaces can be used for the development of intelligent power cable sensors.

In this study, a significant attenuation of sensing signals by the cable's copper shielding and semiconductive layers was observed. Configurations 2 and 4–8 in the experiment showed that capacitive coupling without modification did not yield distinct localization peaks due to direct reflection artifacts and shielding-induced suppression.[31] Noninvasive sensors that can penetrate or bypass metallic shielding by using high-frequency coupling mechanisms must be designed. The integration of HFCT and capacitive coupling after removing the shielding layer can attain a balance between SNR and transmission speed, which serves as a reference for the hybrid sensor approach.

The shift from TDR and BIS to FMCW enables an advancement in sensor resolution. While TDR is susceptible to interference, using FMCW enables the translation of longitudinal delays into frequency differences to ensure superior noise immunity in energized environments.[32] The identification of thermal aging defects with an error of 5.10% enables FMCW sensors to provide the high-resolution data necessary for preventive maintenance. This underscores the potential for FMCW-based sensors to become a standard for real-time, high-fidelity monitoring in smart grids.

Active sensing is essential in monitoring operating conditions. Existing systems require scheduled power outages, which are difficult to arrange in urban areas. Therefore, the ring-shaped capacitive electrode is required for noninvasive signal injection to make sensors interact with high-voltage conductors safely.[33] The implementation of data processing modules accounts for the impedance of connected grid equipment, such as transformers and busbars, and enables the adaptive sensors to recalibrate them in accordance with the real-time grid conditions.[34]

The deviation between experimental and theoretical results suggests that environmental factors and coupling mechanisms introduce minor spectral distortions. Therefore, it is necessary to refine the single- and dual-cycle mixing algorithms to optimize the balance between spectral smoothness and noise immunity. By miniaturizing the capacitive coupling hardware, sensors can be deployed on a large scale for underground distribution networks.

For the developed system to be widely adopted, a specialized software interface must be developed for signal processing. The raw frequency-domain data, which contains complex interference patterns and reflections, is processed through an automated peak-tracking algorithm.

To ensure the proposed system is accessible to those who might not be familiar with reflectometry, the hardware needs to be designed to interface with a simplified digital dashboard. The hardware needs to feature complex frequency-domain spectra and notch features processed by an automated peak-tracking algorithm to enhance user-friendliness. Instead of requiring manual interpretation of the reflection coefficient, the highest-magnitude impedance discontinuity must be automatically identified to convert the frequency-modulated beat signal

into a linear distance (in meters) and to locate the precise locations of defects on a simplified cable diagram.

The depth and interval of the spectral notches must be measured to estimate the health index of the cable. This translates numerical data into a traffic-light status.[35] By pairing the diagnostic unit with a mobile tablet's GPS, the detected defect location can be shown on a GIS map. This will assist nonspecialists in physically locating the exact buried or overhead cable segment requiring maintenance.[36] This automated approach eliminates the need for specialized signal analysis, making high-resolution FMCW technology a practical tool for routine grid maintenance.

To enhance usability for field technicians, the developed system incorporates a graphical interface that displays defect localization results on a PC or tablet. The interface automatically converts spectral notch positions into cable distance values, highlighting defect locations with color-coded severity indicators. This design eliminates the need for specialized signal-processing knowledge, enabling practical deployment in routine maintenance workflows.

6. Conclusions

We proposed an online localization method for partial insulation defects in power distribution cables under live operating conditions, using FMCW and capacitive coupling. We applied the method to examine signal transmission characteristics, optimization strategies, and matched filtering techniques and revealed the mechanisms and key challenges of signal propagation under capacitive coupling.

The experiment results showed that terminal reflection peaks were masked by interference signals reflected from the coupling capacitor, resulting in localization failure. The issue was caused by the strong attenuation of the electric field by the copper shielding layer, which suppressed the signal energy transmitted from the core conductor. Transmission performance was improved significantly through structural optimization, in which the insulation, copper shielding, and semiconductive layers were stripped at the coupling points. Under these conditions, capacitive coupling and HFCT injection methods accurately extracted time differences corresponding to internal signal transmission. Capacitive coupling achieved a time difference of 574.4 ns (101.26 m, *error* <1.3%), while HFCT injection yielded 548.7 ns (96.74 m, *error* <3.3%). Subsequent online localization experiment results showed distinctive notch characteristics in the spectral domain at multiple frequency bands. The average localization error was 5.63% for both 40 and 50 MHz sweeps. Adoption of the single-cycle signal mixing method produced smoother spectral curves and improved notch distinguishability, although with reduced noise immunity. For a 64 m cable containing a 2 m thermal aging defect at the 41 m position, the system identified the defect with a relative error of 5.10% (969 Hz deviation). Multiple notch peaks were observed, corresponding to the defect length, thereby demonstrating the method's capability to characterize defect severity.

Although the reported 5.1% error translates to 326 m in a 6.4 km line, practical deployment involves sectional testing of cable spans (50–200 m), reducing the effective localization error to a range suitable for repair crews. Furthermore, the detection performance of the system is

influenced by defect severity: larger defects generate stronger reflections and clearer notch features, whereas incipient defects yield weaker signals that require advanced processing. Future research will focus on quantifying this relationship to establish defect severity thresholds to enable reliable preventive maintenance.

The implementation of a ring-shaped capacitive electrode enabled high-fidelity signal injection while blocking power-frequency voltages. The results of comparing capacitive and HFCT sensors can be used to enhance the viability of hybrid sensing chains for energized environments. The proposed system showed a 2.2% error in frequency shift, confirming that FMCW-based sensors provide superior noise immunity and diagnostic range compared with conventional BIS. The data processing module that accounts for equipment impedance can be used for active sensing, maintaining high SNRs under electromagnetic interference, and enabling preventive maintenance before full insulation breakdown.

The integration of FMCW technology with capacitive coupling hardware provides a robust, noninvasive solution for live cable monitoring. The proposed method advances cable diagnostics and offers broad applications for smart grid applications. It is required to enhance the defect-type identification ability of the proposed system by extending multidevice coupling modeling and refining adaptive algorithms. Then, the system will improve the engineering applicability and commercial scalability of advanced diagnostic sensors. While we addressed the problem of high-resolution signal injection into energized shielded cables, the solution might be limited to single-core distribution cables. Therefore, further studies are needed to mitigate signal attenuation in longer cable runs and develop automated defect classification algorithms to enhance field-readiness for maintenance technicians.

References

1 J. Liu, M. Ma, X. Liu, and H. Xu: Sensors **24** (2024) 3067. https://doi.org/10.3390/s24103067
2 B. Shan. S. Du. H. Cheng, and C. Li: Polymers **14** (2022) 5478. https://doi.org/10.3390/polym14245478
3 R. Xianjie, X. Zhonglin, D. Yuqin, H. Xiaoyu, and Z. Kai: Trans. China Electrotech. Soc. **40** (2025) 1628. https://eurekamag.com/research/096/692/096692278.php?utm_source=copilot.com
4 M. C. Lança, M. Fu, E. Neagu, L. A. Dissado, J. Marat-Mendes, A. Tzimas, and S. Zadeh: J. Non-Cryst. Solids **383** (2007) 47. https://doi.org/10.1016/j.jnoncrysol.2007.03.035
5 S. J. Zhao, L. T. Gong, B. B. Zhan, W. Wang, and C. R. Li: High Volt. Eng. **49** (2023) 2121. https://doi.org/10.13336/j.1003-6520.hve.20221489
6 Z. Cheng, H. Mu, X. Zou, C. Song, R. Wang, and K. Fan: IEEE Trans. Dielectr. Electr. Insul. Early Access (2025) 1. https://doi.org/10.1109/TDEI.2025.3625111
7 H. S. Zhao, J. J. Sun, and X. D. Xu: Power Syst. Technol. **46** (2022) 4548. https://doi.org/10.13335/j.1000-3673.pst.2021.2541
8 B. L. Han, S. N. Li, X. Yang, W. Wang, and C. R. Li: Trans. China Electrotech. Soc. **36** (2021) 4809. https://doi.org/10.19595/j.cnki.1000-6753.tces.210871
9 N. Hirai, T. Yamada, and Y. Ohki: Proc. 2012 IEEE Int. Conf. Condition Monitoring and Diagnosis, Bali, Indonesia (IEEE, 2012) 229. https://doi.org/10.1109/CMD.2012.6416417
10 S. Zhao, L. Gong, B. Zhan, C. Liang, W. Wang, and C. Li: Proc. CSEE **43** (2023) 4452. https://doi.org/10.13334/j.0258-8013.pcsee.221254
11 S. J. Zhao, B. B. Zhan, L. T. Gong, W. Wang, C. R. Li, and X. K. Meng: Trans. China Electrotech. Soc. **38** (2023) 3009. https://doi.org/10.19595/j.cnki.1000-6753.tces.221790
12 C. Son, H. Cheon, H. Lee, D. Kang, and J. Park: J. Sens. Sci. Technol. **32** (2023) 219. https://doi.org/10.46670/JSST.2023.32.4.219
13 H. Kim, H, Jeong, H. Lee, and S. W. Kim: Sensors **21** (2021) 5936. https://doi.org/10.3390/s21175936
14 S. Hu, L. Wang, C. Gao, B. Zhang, Z. Liu, and S. Yang: Sensors **18** (2018) 3724. https://doi.org/10.3390/s18113724

15 C. Furse, Y. C. Chung, R. Dangol, M. Nielsen, G. Mabey, and R. Woodward: IEEE Trans. Electromagn. Compat. **45** (2003) 306. https://doi.org/10.1109/TEMC.2003.811305
16 M. K. Smail, T. Hacib, L. Pichon and F. Loete: IEEE Trans. Magn. **47** (2011) 1502. https://doi.org/10.1109/TMAG.2010.2089503
17 W. Zhu, B. Hui, J. Li, T. Han, L. Zhao, and S. Hou: Energies **18** (2025) 5346. https://doi.org/10.3390/en18205346
18 N. Giaquinto, M. Scarpetta, and M. Spadavecchia: IEEE Trans. Instrum. Meas. **69** (2020) 7271. https://doi.org/10.1109/TIM.2020.2974110
19 B. Wang, S. Li, J. Peng, J. Deng, X. Zhao, and H. Sun: IEEE Trans. Instrum. Meas. **74** (2025) 3544511. https://doi.org/10.1109/TIM.2025.3579848
20 A. Hajjafari, R. Badiei, H. Asharioun, and R. Nasiri: Proc. 2023 Int. Conf. Protection and Automation of Power Systems (IPAPS, 2023) 1. https://doi.org/10.1109/IPAPS58344.2023.10123324
21 M. Fritsch and M. Wolter: IEEE Trans. Instrum. Meas. **71** (2022) 9004309. https://doi.org/10.1109/TIM.2022.3177189
22 C. Gao, L. Wang, J. Mao, S. Hu, B. Zhang, and S. Yang: IEEE Trans. Power Deliv. **34** (2019) 1684. https://doi.org/10.1109/TPWRD.2019.2918173
23 F. Fu, X. Yang, L. Cheng, L. Wang, J. Zhang, and Z. Pan: J. Phys. Conf. Ser. **1303** (2019) 012098. https://doi.org/10.1088/1742-6596/1303/1/012098
24 J. Wang, J. Li, C. Peng, Z. Wu, D. Ju, and Q. Zhang: Micromachines **15** (2024) 1314. https://doi.org/10.3390/mi15111314
25 P. Zhang, C. Yao, L. Yu, X. Zhao, L. Zhao, L. Lan, and S. Dong: High Vol. **8** (2022) 550. https://doi.org/10.1049/hve2.12261
26 W. Ben Hassen, M. Slimani, and F. Auzanneau: Meas. Sens. **43** (2026) 101981. https://doi.org/10.1016/j.measen.2025.101981
27 Y. H. Lee, S. S. Bang, C.-K. Lee, G.-Y. Kwon, G. H. Ji, and Y.-J. Shin: Proc. IEEE 2nd Int. Conf. Dielectrics (ICD, 2018) 1. https://doi.org/10.1109/ICD.2018.8514783
28 H.-P. Park, G.-Y. Kwon, C.-K. Lee, and S. J. Chang: Measurement **238** (2024) 115188. https://doi.org/10.1016/j.measurement.2024.115188
29 L. Wang, C. Ma, L. Zhu, X. Wang, C. Yin, H. Cong, and T. Shi: IET Gener. Transm. Distrib. **16** (2022) 2331. https://doi.org/10.1049/gtd2.12450
30 Z. Yu, X. Wang, M. Fang, and S. Zhang: Proc. Int. Conf. Advances in Electrical Engineering and Computer Applications (AEECA, 2024) 189. https://doi.org/10.1109/AEECA62331.2024.00041
31 H. Lim, G.-Y. Kwon, and Y.-J. Shin: IEEE Trans. Instrum. Meas. **70** (2021) 1. https://doi.org/10.1109/TIM.2021.3092514
32 W. Zhu, B. Hui, J. Li, T. Han, L. Zhao, and S. Hou: Energies **18** (2025) 5346. https://doi.org/10.3390/en18205346
33 A. Ansari, S. Y. Nia, A. Afshari, and S. Mishra: Sci. Rep. **15** (2025) 41230. https://doi.org/10.1038/s41598-025-25080-7
34 H. Su, H. Li, W. Liang, C. Shen, and Z. Xu: Sensors **24** (2024) 388. https://doi.org/10.3390/s24020388
35 C. Retzlaff, O. Gollob, C. Nothdurft, A. Stampfer, and K. Orge: Croat. J. For. Eng. **46** (2017) 11. https://doi.org/10.5552/crojfe.2025.3270
36 M. Wang and X. Yin: Autom. Constr. **141** (2022) 104464. https://doi.org/10.1016/j.autcon.2022.104464